doi:10.1093/brain/awr030 Brain 2011: 134; 1168–1183 | 1168

BRAIN
A JOURNAL OF NEUROLOGY

Human neural progenitors from different foetal forebrain regions remyelinate the adult mouse spinal cord

Delphine Buchet,[1,2,3] Corina Garcia,[1,2,3] Cyrille Deboux,[1,2,3] Brahim Nait-Oumesmar[1,2,3,4] and Anne Baron-Van Evercooren[1,2,3,4]

1 Université Pierre et Marie Curie-Paris 6, Centre de Recherche de l'Institut du Cerveau et de la Moelle Epinière, UMR-S975, Paris, France
2 Inserm, U975, Paris, France
3 CNRS, UMR 7225, Paris, France
4 AP-HP, Hôpital Pitié-Salpêtrière, Fédération de Neurologie, Paris, France

Correspondence to: Anne Baron-Van Evercooren
Batiment ICM, 5ème étage, pièce 5.031,
Centre de Recherche de l'Institut du Cerveau et de la Moelle Epinière,
UPMC-Paris 6, UMR_S 975; Inserm U 975; CNRS UMR 7225,
47 bd de l'Hôpital,
75651 Paris Cedex 13, France
E-mail: anne.baron@upmc.fr

Improving oligodendroglial differentiation from human foetal neural progenitor cells remains a primordial issue to accomplish successful cell-based therapies in myelin diseases. Here, we combined *in situ*, *in vitro* and *in vivo* approaches to assess the oligodendrogenic potential of different human foetal forebrain regions during the first trimester of gestation. We show for the first time that the initial wave of oligodendrocyte progenitor emergence in the ventral telencephalon onsets as early as 7.5 weeks into gestation. Interestingly, *in vitro*, isolation of ganglionic eminences yielded oligodendrocyte progenitor-enriched cultures, as compared with cortex and thalamus. Most importantly, single injection of human neural progenitors into rodent models of focal gliotoxic demyelination revealed the great capacity of these cells to survive, extensively migrate and successfully remyelinate the spinal cord, irrespective of their origin. Thus, our study brings novel insights into the biology of early human foetal neural progenitor cells and offers new support for the development of cellular therapeutics for myelin disorders.

Keywords: human neural progenitor cells; oligodendrocyte; migration; oligodendrogenesis; remyelination

Abbreviations: GFAP = glial fibrillary acidic protein; hNPC = human foetal neural progenitor cell; MBP = myelin basic protein

Introduction

Neural stem cells are a promising tool for cell replacement in various neurological disorders, including diseases that manifest with myelin failure or loss, such as multiple sclerosis or some leucodystrophies. The proliferative properties of these cells, as well as their ability to generate the major cell types of the CNS, including myelinating oligodendrocytes, have enabled the validation of their regenerative potential in a variety of demyelinating models (Chandran *et al*., 2008; Duncan, 2008; Goldman *et al*., 2008; Tepavcevic and Baron-Van Evercooren, 2008; Martino *et al*., 2010).

However, the difficulty to derive and amplify human oligodendrocyte progenitor cells from immature neural stem/progenitor cells (Quinn *et al*., 1999; Roy *et al*., 1999; Zhang *et al*., 2000; Buchet *et al*., 2002*a*; Chandran *et al*., 2004), especially when isolated during early foetal development, has long hampered

Received June 28, 2010. Revised November 26, 2010. Accepted December 27, 2010

successful remyelination attempts in these models (Buchet and Baron-Van Evercooren, 2009). This limitation was due, at least in part, to the fact that protocols of epigenetic stimulation known to promote rodent neural stem cell commitment towards the oligodendroglial lineage have proven inefficient in humans (Murray and Dubois-Dalcq, 1997; Zhang *et al*., 2000). As a result, various strategies have been explored to enhance the myelinating potential of neural stem and progenitor cells. One of these consisted of selecting early glial progenitor cells from human tissue, based on their expression of membrane markers (Roy *et al*., 1999; Windrem *et al*., 2004, 2008). Thus, A2B5$^+$/PSA-NCAM$^-$ progenitors isolated from second trimester foetal neural tissue were shown to extensively myelinate the congenitally dysmyelinated CNS of newborn myelin basic protein (MBP)-deficient 'shiverer' mice, as well as to re-establish normal axonal conduction and prolong the otherwise shortened life-span of the animals (Windrem *et al*., 2008). Recently, another strategy was developed that consisted of promoting the commitment of human foetal neural progenitor cells (hNPCs) towards the oligodendroglial lineage by genetic stimulation (Maire *et al*., 2009). Over-expression of the transcription factor Olig2 induced oligodendrocyte progenitor cell specification from transduced hNPCs *in vitro*, and a 2-fold increase in oligodendroglial differentiation after grafting into 'shiverer' mouse brain. A third strategy would consist of defining a CNS region that may be enriched in putative oligodendrocyte progenitor cells during early foetal development. In the present work, we focused on this latter strategy and evaluated the oligodendroglial potential of foetal hNPCs isolated from different parts of the forebrain during the first trimester of gestation.

In rodents, the sequence of forebrain oligodendrocyte progenitor cell specification has been well described (Spassky *et al*., 1998; Kessaris *et al*., 2006). A first wave of oligodendrocyte progenitor cell emergence takes place around embryonic Day 12.5 in the medial ganglionic eminences and entopeduncular area (Spassky *et al*., 1998). By that time, most oligodendrocyte progenitor cells are concentrated in well-defined parts of the ventral forebrain and have not yet dispersed throughout lateral and dorsal areas. A second wave of oligodendrocyte progenitor cell emergence takes place around embryonic Day 15 in the lateral ganglionic eminences, followed by a third wave that appears dorsally in the cortex after birth. Each of these waves give rise to distinct oligodendrocyte progenitor cell populations that can be distinguished from one another by the initial expression of homeobox genes that sign their territorial origins (Kessaris *et al*., 2006). However, the functional homology between these oligodendrocyte progenitor cell populations is still a matter of debate (Richardson *et al*., 2006).

In humans, numerous similarities were highlighted with rodent forebrain development. In particular, colocalization of early oligodendrocyte progenitor cell markers with homeobox genes suggested that, as in rodents, human oligodendrocytes originate from at least three distinct areas of the forebrain, including the medial and lateral ganglionic eminences and cortical ventricular zone (Rakic and Zecevic, 2003). However, until now, most of the developmental studies focusing on oligodendrocyte progenitor cell emergence in the human forebrain have been conducted either at very early stages of development when oligodendrocyte progenitor cells cannot yet be detected (Jakovcevski and Zecevic, 2005*a*), or on second trimester foetuses, between 15 and 23 weeks of gestation, by which time oligodendrocyte progenitor cells have already colonized ventral and dorsal territories (Back *et al*., 2001; Rakic and Zecevic, 2003; Jakovcevski and Zecevic, 2005*a*, *b*; Jakovcevski *et al*., 2009). Thus, there appears to be a gap in brain development description during the first trimester of gestation, and the switch from neurogenesis to oligodendrogenesis that takes place around embryonic Day 12.5 in the rodent forebrain has not yet been well dated in humans.

Understanding the time course of oligodendrocyte emergence within the human developing brain, as well as the events leading to oligodendrocyte differentiation and myelination, remains a key issue for successful therapies. In the present study, we combined multiple approaches to assess the oligodendrogenic potential of different human forebrain regions. Reverse transcription-polymerase chain reaction and immunohistochemical analysis performed on human foetal brain tissue allowed for the characterization of the spatio-temporal onset of oligodendrogenesis during early human gestation. Moreover, isolation of cells from cortex, ganglionic eminences and thalamus allowed enrichment of putative early oligodendrocyte progenitor cells *in vitro*. Finally, we demonstrated that, after amplification, hNPCs from these three regions displayed great propensities to survive, migrate and generate large amounts of myelinating oligodendrocytes when grafted into two different mouse models of spinal cord focal demyelination.

Materials and methods

Tissues

Human foetuses were obtained after legal abortion according to the recommendations of the Agence de la Biomedecine (agreement #003187) with the written consent of the patients. The samples were aged as follows: 6.5 ($n = 1$), 7.5 ($n = 2$), 8.5 ($n = 2$) and 9 ($n = 1$) weeks of gestation as determined by crown-to-rump length measurement by ultrasound scanning and by observation of development of the fingers and toes. The collection procedure was performed as previously described (Buc-Caron, 1995). Supplementary Table 1 summarizes the experimental use of the different foetuses.

Cell culture

Primary cultures were initiated from the cortex, ganglionic eminences and thalamus of three independent foetuses. Briefly, after removal of the meninges and fine dissection of the regions of interest, each region was cut into small pieces and single cell suspensions were obtained by incubation in ATV buffer (consisting of 0.05% trypsin, 0.1% glucose and 0.5 nM EDTA) for 20 min at 37°C, followed by mechanical trituration.

Short-term characterization

Dissociated cells from cortex, ganglionic eminences and thalamus were immediately seeded in 24-well plates (5×10^4 cells/well) on glass coverslips coated with polyornithin (Sigma-Aldrich) and laminin (Sigma-Aldrich) in NEF medium [consisting of a 1:1 mixture of

Dulbecco's modified Eagle's medium-F12 (Invitrogen) supplemented with 1% N2 supplement (Invitrogen); 0.5% B27 (Invitrogen); 25 μg/ml insulin (Sigma-Aldrich); 6 mg/ml glucose (Sigma-Aldrich); 5 mM HEPES (Invitrogen); 20 ng/ml basic fibroblast growth factor (Sigma-Aldrich) and 20 ng/ml epidermal growth factor (Sigma-Aldrich)]. After 5 days, cells were fixed in 4% paraformaldehyde (Sigma-Aldrich).

Amplification

Dissociated cells from the cortex, ganglionic eminences and thalamus were seeded at the density of 10^6 cells/T75 flask in 10 ml NEF medium. Fresh medium was added twice a week. Long-term amplification was performed by successive passages every 2–3 weeks, depending on the size of the spheres and growth rate of each region. At each passage, spheres from each region were dissociated in ATV and re-seeded at the density of 10^6 cells/T75 flask in 10 ml NEF medium.

Long-term characterization

Cells were amplified as described above for 100 days *in vitro* (P8–P9), dissociated in ATV, seeded in 24-well plates (5×10^4 cells/well) and further processed as for short-term characterization.

Demyelination and transplantation

Demyelination and transplantation in nude mice

Adult Swiss nude mice (8–10 weeks of age; Janvier) were anaesthetized by intraperitoneal injection of a mixture of 150 mg/kg ketamine (Alcyon) and 150 mg/kg xylazine (Alcyon). Focal demyelination was performed in 48 animals by single injection of 1 μl of 1% lysolecithin (Sigma-Aldrich) into the dorsal funiculus of the spinal cord of each animal at the level of the 13th thoracic vertebrae. Forty-eight hours after lysolecithin injection, 1 μl of cell suspension (10^5 cells/μl) from cortex, ganglionic eminences and thalamus was injected at the site of demyelination. Transplantation studies were performed with hNPCs from two independent foetuses. Twenty-four animals were used for each foetus, divided into three groups of eight animals for each region (cortex, ganglionic eminences and thalamus). Cells were injected after amplification and transduction with the cytomegalovirus-green fluorescent protein (CMV-GFP) lentiviral vector.

Mice were sacrificed at 6 ($n = 6$ per group) and 33–49 weeks post-grafting ($n = 2$ per group) by transcardiac perfusion of 0.9% NaCl (Merck) and 4% paraformaldehyde. After dissection, spinal cords were cryopreserved in 15% sucrose-1× phosphate buffered saline overnight. They were then included in 7% gelatin (Merck)-15% sucrose (Sigma-Aldrich)-1× phosphate buffered saline, frozen in cold isopenthane at –60°C and stored at –80°C until use. Thick sections of 12 μm were cut with a cryostat (Leica) and used for immunohistochemistry.

Demyelination and transplantation in 'shiverer' mice

Adult 'shiverer' mice (BalbC strain; 8 weeks of age) were demyelinated and transplanted following the same procedure as described above. For this series of experiments, 0.5 μl of cell suspension (10^5 cells/μl) from cortex, ganglionic eminences and thalamus were grafted after amplification *in vitro* ($n = 10$ per region), but without previous lentiviral transduction. Mice were immunosuppressed by daily injection of 20 mg/kg cyclosporine A (Sandimmun) and sacrificed at 10.5 weeks post-grafting. For immunohistochemistry, tissues were processed as described above ($n = 4$ per group and per region). For electron microscopy, mice were perfused with 0.9% NaCl followed by a mixture of 4% paraformaldehyde/2.5% glutaraldehyde (Electron Microscopy Science) in 1× phosphate buffered saline for 45 min ($n = 4$ per group and per region).

Immunochemistry

Immunocytochemistry

Human cell characterization was performed using the following primary antibodies: anti-human Nestin (1:1000; clone Nestin 24, Covance); anti-Olig2 (1:500, Chemicon AB9610); anti-β3-tubulin (1:800, Sigma-Aldrich); anti-MAP5 (1:200, clone AA6, Sigma-Aldrich); A2B5 (1:5 mouse IgM hybridoma from ATCC); O4 (1:5, mouse IgM hybridoma from ATCC) and anti-glial fibrillary acidic protein (GFAP; 1:500, Dako). Cells were then incubated for 10 min in Hoechst dye (1 μg/ml Sigma-Aldrich) and with the corresponding secondary antibodies.

Immunohistochemistry

Human cells transplanted in nude mice were identified according to their native expression of GFP, or with an antibody directed against GFP (1:500, Interchim). The phenotype of GFP^+ human cells was determined by immunohistochemistry using the following antibodies: anti-human nestin (1:1000, Covance), anti-APC (CC1, 1:100, Invitrogen 51-2700), anti-human NOGO-A (1:100, Santa Cruz Biotechnology), anti-MBP (1:400, Chemicon), anti-Sox10 (1:50, R&D Systems), anti-Olig2 (1:500, Chemicon), anti-human GFAP (SMI21, 1:1000, Covance), anti-human Tau (Tau13, 1:1000, Covance) and anti-NeuN (1:100, Millipore). The proliferation of the grafted human cells was assessed by Ki67 (1:200, Dako) staining. 'Shiverer' white matter was visualized by myelin oligodendrocyte glycoprotein (MOG) staining (1:200, ascite obtained from Dr Linnington, Edinburgh, UK). Paranodes were identified by Caspr (1:800, generous gift from E. Peles, Rehovot, Israel) staining. Clustering of Na_v channels was assessed by pan-Na_v (1:100, Sigma) staining. For MBP and MOG staining, slices were pretreated with ethanol (10 min at room temperature). For Caspr and pan-Na_v staining, slices were incubated in methanol (10 min at −20°C) and saturated in the presence of 0.1% glycine (Research Organics). For Olig2, Ki67 and NeuN staining, sections were pre-incubated in boiling citrate buffer (Vector) for 2 min. Sections were incubated for 10 min in Hoechst dye (1μg/ml, Sigma-Aldrich) and then with the corresponding secondary antibodies.

Electron microscopy

After dissection and post-fixation in 4% paraformaldehyde/2.5% glutaraldehyde, 'shiverer' spinal cords were cut in 0.5–1 mm-thick pieces and fixed in 2% osmium tetroxide (Sigma-Aldrich) overnight. After dehydration, samples were embedded in Epon. Ultra-thin sections (80 nm) were examined with a Philips electron microscope.

Statistical analysis

ANOVA analysis was performed among the three regions using the Sigma Stat software. Pairwise comparison was performed using the Dunn's Method.

The methods for reverse transcription-polymerase chain reaction, lentiviral vectors, cell counting and myelination quantification are described in the online Supplementary Material.

Results

The human foetal forebrain undergoes a switch from neurogenesis to oligodendrogenesis during the first trimester of gestation

Sections of 7.5-week-old foetuses were used to characterize the various cell types present in the human forebrain by immunohistochemistry (Fig. 1; Supplementary Fig. 1). At this stage of development, the vast majority of cells expressed Nestin (Supplementary Fig. 1D–F), a marker of neuroepithelial cells and early progenitors, indicating the immaturity of the forebrain. Most Nestin$^+$ cells co-expressed MAP5 (Supplementary Fig. 1D–F) and β3-tubulin, two neuroblast markers, indicating that the forebrain was undergoing neurogenesis. Astrocytes were not detected in either the telencephalon or diencephalon, as revealed by the absence of GFAP immunoreactivity in these regions. In the telencephalon, Olig2$^+$ cells were concentrated in the ventricular and subventricular zones of medial ganglionic eminences (Supplementary Fig. 1E; Fig. 1A, B and F) and entopeduncular area (Fig. 1A, B and G), and to a lesser extent in lateral ganglionic eminences (Fig. 1A and B), but none were detected in the cortex (Supplementary Fig. 1D; Fig. 1A, B and E). Olig2$^+$ cells were also found in the diencephalon, in the thalamus and hypothalamus (Supplementary Fig. 1F; Fig. 1C, D and H). While almost all Olig2$^+$ cells co-expressed MAP5 (Supplementary Fig. 1E and F),

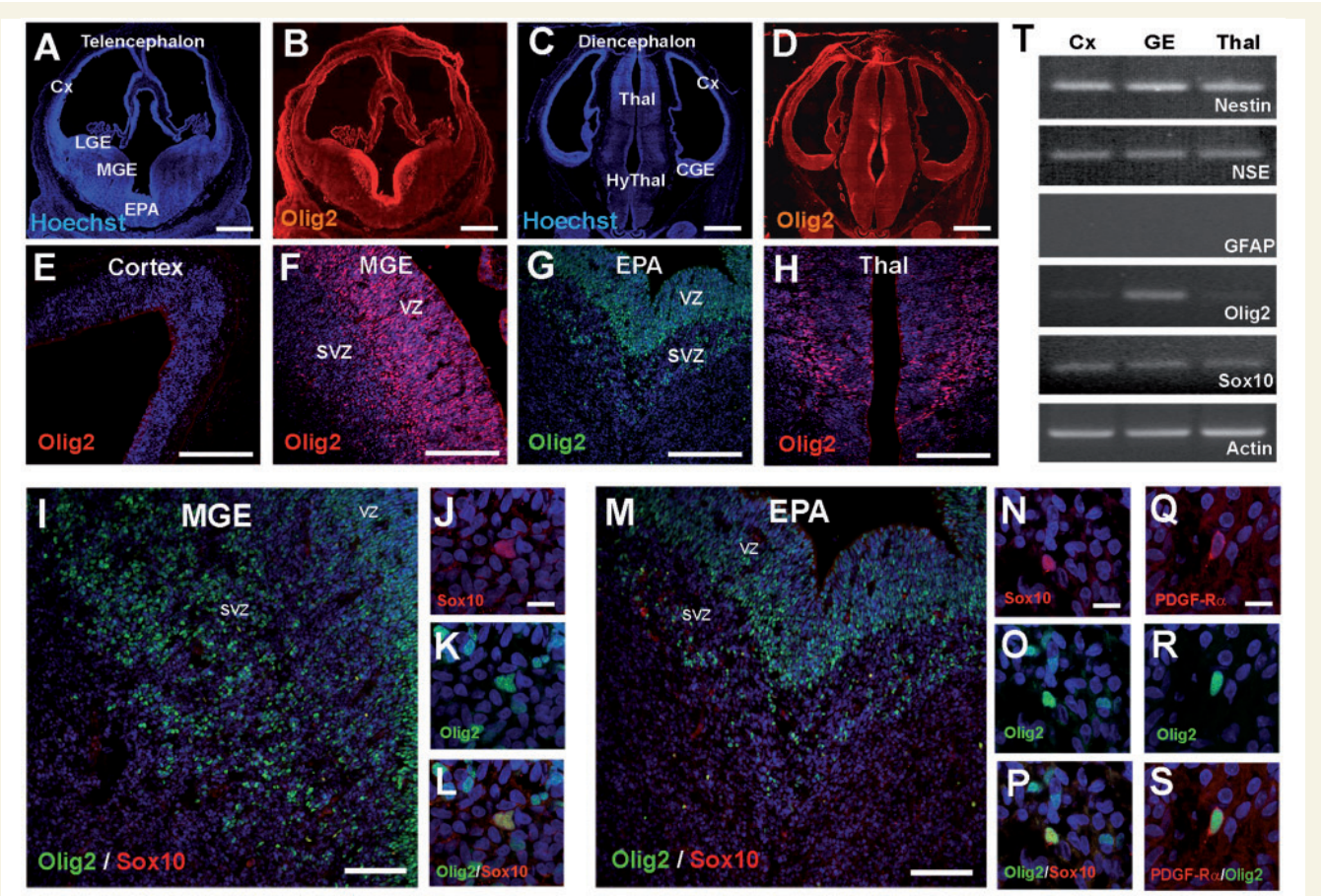

Figure 1 Oligodendrogenesis onsets as early as 7.5 weeks of gestation in the human foetal forebrain. (**A–H**) Immunohistochemical analysis of Olig2 expression pattern performed on forebrain sections of 7.5 week-old foetuses at the telencephalic (**A–B** and **E–G**) and diencephalic (**C–D**, **H**) levels. While Olig2 was absent from cortex (**E**, red), it was massively expressed in medial ganglionic eminences (**F**, red), entopeduncular area (**G**, green) and to a lesser extent in thalamus (**H**, red) and hypothalamus (**D**, red). (**I–S**) Double immunohistochemical staining against Olig2 (green) and the oligodendrocyte progenitor cell-specific markers Sox10 (**I–P**) and platelet derived growth factor receptor α (**Q–S**), showing the emergence of the first oligodendrocyte progenitor cells in the subventricular zone of medial ganglionic eminences (**I–L**) and entopeduncular area (**M–S**). (**T**) Semi-quantitative reverse transcription-polymerase chain reaction performed on snap-frozen tissue from cortex, ganglionic eminences (GE) and thalamus. Nestin and neuron-specific enolase expression in the three regions, as well as GFAP absence of expression, confirmed that the foetal forebrain was undergoing neurogenesis. Although expressed in the three regions, Olig2 and Sox10 transcripts were prominent in ganglionic eminences. PDGF-Rα = platelet derived growth factor receptor alpha; CGE = caudal ganglionic eminences; Cx = cortex; EPA = entopeduncular area; HyThal = hypothalamus; LGE = lateral ganglionic eminences; MGE = medial ganglionic eminences; SVZ = subventricular zone; Thal = thalamus; VZ = ventricular zone. Scale bars: (**A–D**) 1 mm; (**E–H**) 200 μm; (**I** and **M**) 100 μm; (**J**, **N** and **Q**) 10 μm.

indicating their neuroblastic phenotype, a few Olig2$^+$ cells co-expressed the transcription factor Sox10 (Fig. 1I–P) and platelet derived growth factor receptor α (Fig. 1Q–S) in medial ganglionic eminences and entopeduncular area, which identified them as oligodendrocyte progenitor cells. The extremely small number (<0.01%) of these cells, which were found only in these regions and only outside the ventricular zone, combined with the fact that late oligodendrocyte progenitor cell markers such as NG2 and O4 were not expressed, indicated that oligodendrogenesis was at its very beginning. Thus, although the human forebrain was undergoing neurogenesis, our data highlight that oligodendrocyte progenitor cell specification onsets in the ventral telencephalon as early as 7.5 weeks of gestation.

The phenotype of the forebrain cells was also characterized by reverse transcription-polymerase chain reaction performed on RNA extracts from cortex, ganglionic eminences and thalamus tissue (Fig. 1T). Nestin and neuron-specific enolase transcripts were expressed in the three regions, confirming the presence of neuroepithelial cells and neuroblasts, and GFAP transcripts were not expressed, consistent with the immunohistochemical analysis. Interestingly, Olig2 and Sox10 transcripts were present in the three regions, whereas the proteins were expressed only in ventral telencephalon. However, consistent with the high expression of Olig2 protein in ganglionic eminences, semi-quantitative analysis indicated that Olig2 transcripts were expressed at a much higher level (~14-fold) in ganglionic eminences than in cortex and thalamus.

Phenotypic characteristics of cortex, ganglionic eminences and thalamus cells are maintained *in vitro* after isolation from the human foetal forebrain

The phenotype of hNPCs from the various regions was further characterized by RT-polymerase chain reaction and immunocytochemistry on dissociated cells from cortex, ganglionic eminences and thalamus. After 5 days *in vitro*, hNPCs from the three regions mainly consisted of Nestin$^+$ neuroepithelial-like cells (47.3 ± 0.9, 51.6 ± 1.1 and 22.4 ± 2.1% in cortex, ganglionic eminences and thalamus, respectively) (Table 1; Supplementary Fig. 2A–C) and β3-tubulin$^+$ neuroblasts (67.3 ± 1.1, 47.0 ± 1.2 and 69.5 ± 2.1% in cortex, ganglionic eminences and thalamus, respectively) (Table 1; Supplementary Fig. 2G–I). Cells from thalamus displayed a more mature phenotype than cells from cortex and ganglionic eminences, with a lower proportion of Nestin$^+$ cells and a higher proportion of MAP5$^+$ cells (73.7 ± 1.7% in thalamus versus 53.0 ± 1.1 and 47.1 ± 1.1% in cortex and ganglionic eminences, respectively), as well as a lower proportion of proliferating cells (14.0 ± 2.0% of Ki67$^+$ cells in thalamus versus 23.4 ± 1.1 and 32.5 ± 1.3% in cortex and ganglionic eminences, respectively) (Table 1; Supplementary Fig. 2D–F). No GFAP$^+$ astrocytes and only rare (<0.01%) O4$^+$ oligodendrocytes (Supplementary Fig. 2J–L) were detected in cortex, ganglionic eminences and thalamus cultures. Moreover, Olig2$^+$ cells were mainly concentrated in the ganglionic eminences (32.4 ± 1.5%) whereas they were very few in cortex and thalamus (1.0 ± 0.2 and 0.4 ± 0.1%, respectively) (Table 1; Supplementary Fig. 2M–O). A2B5$^+$ cells were found in the three regions (5.3 ± 0.4, 3.7 ± 0.3; 19.5 ± 1.6% in cortex, ganglionic eminences and thalamus, respectively) (Table 1; Fig. 2A–J), suggesting the presence of neuroblasts and/or early glial progenitors. Interestingly, in the ganglionic eminences, 83.7 ± 2.4% of A2B5$^+$ cells did not co-express MAP5, whereas the proportions of such single-labelled cells were only 11.6 ± 4.0 and 36.3 ± 4.6% in cortex and thalamus, respectively (Fig. 2K). Therefore, the majority of A2B5$^+$ cells from cortex and thalamus corresponded to neuroblasts, whereas A2B5$^+$ cells from ganglionic eminences mainly corresponded to glial progenitors.

Reverse transcription-polymerase chain reaction analysis of freshly dissociated cells (Fig. 2L) correlated with the *in vitro* data, with Nestin and neuron-specific enolase, but not GFAP (not shown), expressed in the three regions. Noticeably, transcripts of the oligodendroglial lineage, such as Olig2, Olig1 and Sox10, were detected in ganglionic eminences and thalamus, whereas they were expressed at very low (Sox10) or even undetectable

Table 1 *In vitro* characterization of hNPC phenotype after short- and long-term culture

	Nestin (%)	Ki67 (%)	GFAP (%)	β3-Tubulin (%)	A2B5 (%)	Olig2 (%)
Short-term (5 DIV-P0)						
Cx	47.3 ± 0.9[a]	23.4 ± 1.1[a,c]		67.3 ± 1.1[c]	5.3 ± 0.4[a]	1.0 ± 0.2[c]
GE	51.6 ± 1.1[a]	32.5 ± 1.3[a,b]		47.0 ± 1.2[a,b]	3.7 ± 0.3[a]	32.4 ± 1.5[a,b]
Thal	22.4 ± 2.1[b,c]	14.0 ± 2.0[b,c]		69.5 ± 2.1[c]	19.5 ± 1.6[b,c]	0.4 ± 0.1[c]
Long-term (100 DIV-P7-P8)						
Cx	98.2 ± 0.1	36.7 ± 1.0[a,c]	22.3 ± 0.9[a,c]	2.8 ± 0.3	0.9 ± 0.1[c]	24.9 ± 1.3[a]
GE	98.5 ± 0.1[a]	42.6 ± 1.2[a,b]	5.6 ± 0.5[a,b]	2.1 ± 0.1[a]	3.4 ± 0.2[a,b]	29.1 ± 1.0[a]
Thal	97.7 ± 0.3[c]	24.5 ± 0.8[b,c]	14.7 ± 1.0[b,c]	3.7 ± 0.3[c]	1.2 ± 1.1[c]	4.4 ± 0.4[b,c]

After 5 days *in vitro*, hNPCs from cortex, ganglionic eminences and thalamus consisted mainly of Nestin$^+$ neuroepithelial and β3-tubulin$^+$ neuroblastic cells. Long-term culture enhanced the proportions of Nestin$^+$ and Olig2$^+$ cells in the three regions and decreased the proportions of β3-tubulin$^+$ neuroblasts.
Results are expressed as a percentage of total cells ± SEM.
a Significantly different from thalamus ($P < 0.05$).
b Significantly different from cortex.
c Significantly different from ganglionic eminences.
Cx = cortex; DIV = days *in vitro*; GE = ganglionic eminences; Thal = thalamus.

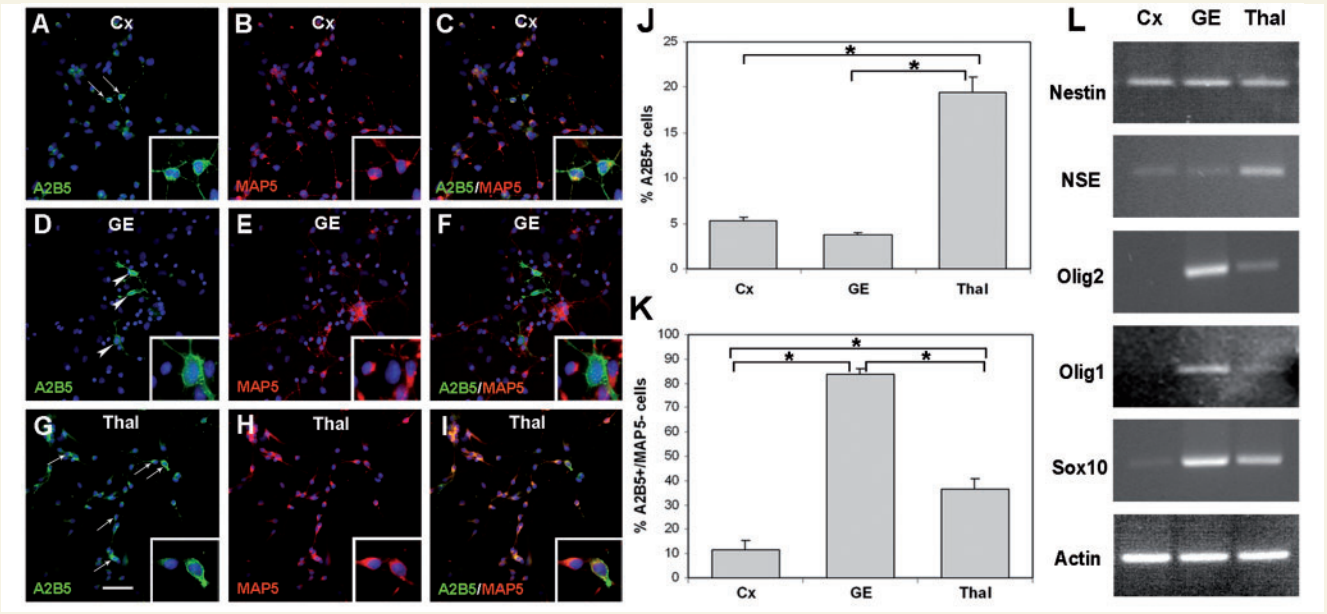

Figure 2 *In vitro,* putative early oligodendrocyte progenitor cells are concentrated in ganglionic eminences, as compared with cortex and thalamus. (**A–I**) Double immunostaining against A2B5 (green) and MAP5 (red) performed on freshly isolated cells from cortex (**A–C**), ganglionic eminences (**D–F**) and thalamus (**G–I**). A2B5$^+$/MAP5$^+$ cells correspond to neuroblasts (arrows), whereas A2B5$^+$/MAP5$^-$ cells correspond to early glial progenitors (arrowheads). (Insets in **A–I**) Magnification of **A–I**. (**J–K**) Proportions of A2B5$^+$ cells (**J**) and A2B5$^+$/MAP5$^-$ cells (**K**) in cortex, ganglionic eminences and thalamus, showing that A2B5$^+$/MAP5$^-$ early glial progenitors were prominent in ganglionic eminences. (**L**) Semi-quantitative reverse transcription-polymerase chain reaction performed on dissociated cells just after dissection from cortex, ganglionic eminences and thalamus, showing that Nestin and neuron-specific enolase RNAs were expressed in the three regions, consistent with early neurogenesis, whereas the oligodendroglial transcripts Olig2, Olig1 and Sox10 were more prominent in ganglionic eminences. *Significantly different from each other (Dunn's test $*P < 0.05$). Cx = cortex; GE = ganglionic eminences; NSE = neuron-specific enolase; Thal = thalamus. Scale bars: (**A–I**) 50 μm.

(Olig1/2) levels in cortex. Semi-quantitative analysis of gene expression indicated that neuron-specific enolase was expressed at higher levels (~2-fold) in thalamus than in cortex and ganglionic eminences. Moreover, Olig2 expression was about 2.6-fold higher in ganglionic eminences than in thalamus, and Sox10 expression was about 4.3-fold higher in ganglionic eminences than in cortex and about 1.5-fold higher in ganglionic eminences than in thalamus, stressing that putative early oligodendrocyte progenitor cells were concentrated in ganglionic eminences.

Long-term amplification *in vitro* enhances the proportion of immature neural cells

In order to obtain large-scale cultures for cell transplantation, primary cultures of hNPCs were initiated from the three regions. Consistent with their more mature initial phenotype, hNPCs from thalamus grew slower than hNPCs from cortex and ganglionic eminences, with fewer and smaller spheres being generated at each passage, and some adherent cells appearing in the flasks (not shown). However, cells from the three regions could be maintained and amplified *in vitro* for at least 100 days. By that time, 36.7 ± 1.0, 42.6 ± 1.2 and 24.5 ± 0.8% of the cells expressed Ki67 in cortex, ganglionic eminences and thalamus, respectively (Table1; Supplementary Fig. 3A–C) and the vast majority of cells from the three regions expressed Nestin (98.2 ± 0.1, 98.5 ± 0.1 and 97.7 ± 0.3% in cortex, ganglionic eminences and thalamus, respectively) (Table 1; Supplementary Fig. 3A–C). A proportion of cells expressed GFAP (22.3 ± 0.9, 5.6 ± 0.5 and 14.7 ± 1.0% in cortex, ganglionic eminences and thalamus, respectively) (Table 1; Supplementary Fig. 3D–F). Virtually all GFAP$^+$ cells expressed Nestin (not shown), indicating that a fraction of the Nestin$^+$ cells corresponded to astrocytes. However, the Nestin$^+$/GFAP$^-$ fraction, which corresponded to immature neuroepithelial-like cells, represented a large majority (75.9, 92.9 and 83.0% in cortex, ganglionic eminences and thalamus, respectively). After amplification *in vitro*, the proportions of neuroblasts were considerably decreased (2.8 ± 0.3, 2.1 ± 0.1 and 3.7 ± 0.3% of β3-tubulin$^+$ cells in cortex, ganglionic eminences and thalamus, respectively) (Table1; Supplementary Fig. 3D–F) and O4$^+$ oligodendrocytes were no longer detected. As compared with short-term characterization, the proportion of A2B5$^+$ cells in long-term cultures was decreased by 5.9- and 16.2-fold in cortex and thalamus, respectively (with 0.9 ± 0.1 and 1.2 ± 1.1% of A2B5$^+$ cells, respectively), whereas it was maintained in ganglionic eminences (with 3.4 ± 0.2% of A2B5$^+$ cells) (Table1; Supplementary Fig. 3G–I). Finally, Olig2 expression was unchanged in ganglionic eminences (29.1 ± 1.0%), whereas it was upregulated in cortex (24.9 ± 1.3%) and thalamus

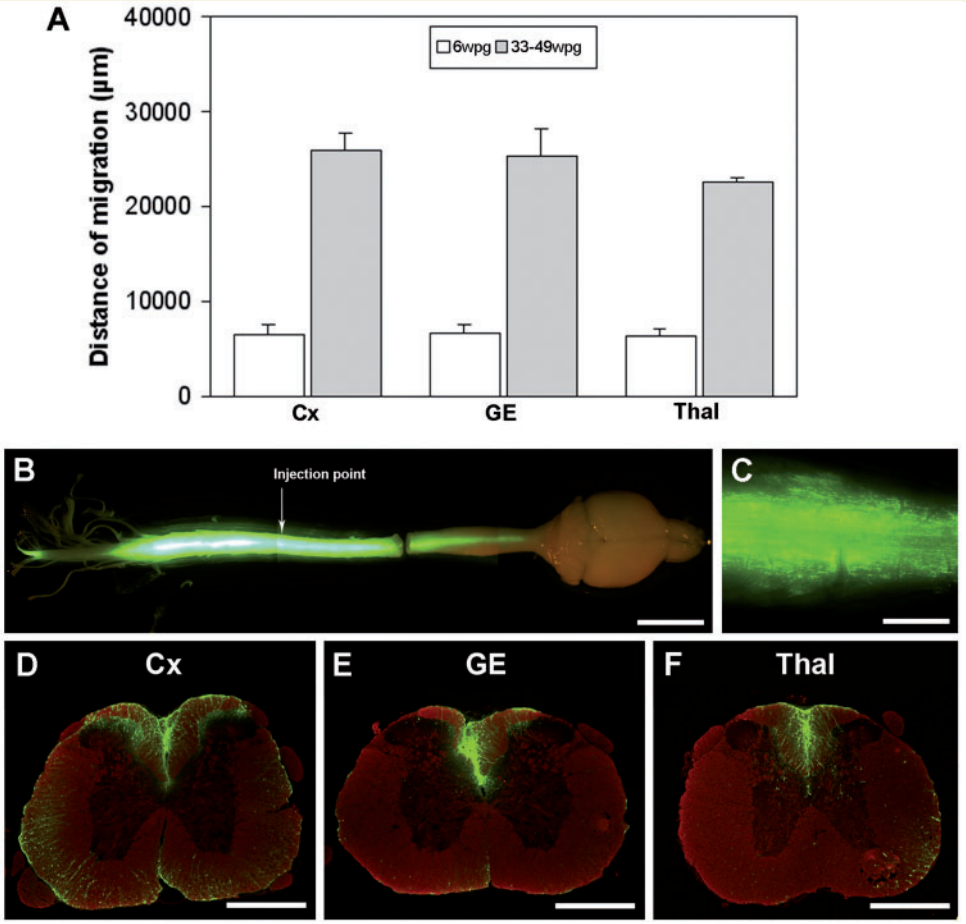

Figure 3 Human foetal neural progenitor cells from cortex (Cx), ganglionic eminences (GE) and thalamus (Thal) display widespread migration after a single injection into the demyelinated spinal cord of nude mice. (**A**) Distance of hNPC migration, estimated as the distance between the most rostral and the most caudal GFP$^+$ cells at 6 and 33–49 weeks post-grafting. (**B**) At 33–49 weeks post-grafting, GFP$^+$ human cells colonized almost the entire spinal cord. (**C**) Magnification of **B** showing GFP$^+$ human cells dispersed within the dorsal funiculus. (**D–F**) Coronal sections from the three groups, showing GFP$^+$ human cells in both dorsal and ventral white matter, and to a lesser extent in the grey matter. White matter is visualized by MOG staining (red). wpg = weeks post-grafting. Scale bars: (**B**) 5 mm; (**C–F**) 500 µm.

(4.4 ± 0.4%) (Table 1; Supplementary Fig. 3J–L). Thus, long-term amplification of hNPCs from the three regions induced enrichment in immature cells, as well as a decrease in neuronal cells and, most interestingly, an increase in Olig2$^+$ cells.

Human foetal neural progenitor cells display long-term survival and widespread migration after transplantation into demyelinated spinal cord

In vivo approaches were then used to assess the remyelinating abilities of hNPCs from the three forebrain regions. After amplification *in vitro*, cells from cortex, ganglionic eminences and thalamus were transduced with a lentiviral vector encoding GFP. The proportions of GFP$^+$ cells were 92.8 ± 0.8, 85.3 ± 2.6 and 95.6 ± 0.6% of the total hNPCs in cortex, ganglionic eminences and thalamus, respectively, indicating very high transduction efficiency (Supplementary Fig. 4). Transduced cells were then transplanted into the demyelinated adult nude mouse spinal cord and animals were sacrificed 6 and 33–49 weeks later for short- and long-term analysis of hNPC fate *in vivo*. Human GFP$^+$ cells were found in all transplanted animals at all time points, indicating that they survived in the host environment for almost 1 year. At 6 weeks post-grafting, proliferation was considerably reduced, as estimated by the proportion of Ki67$^+$ cells among the GFP$^+$ cell population (0.4 ± 0.3, 0.8 ± 0.4 and 2.3 ± 0.7% in cortex, ganglionic eminences and thalamus, respectively), and had completely stopped by 33–49 weeks post-grafting.

Interestingly, grafted hNPCs from the three regions displayed a high migratory potential within the mouse spinal cord (Figs 3 and 4). At 6 weeks post-grafting, GFP$^+$ cells had already consistently migrated from the injection site (estimated distance of migration: 6.5 ± 1.1, 6.8 ± 0.7 and 6.3 ± 0.8 mm in cortex, ganglionic eminences and thalamus groups, respectively) (Figs 3A and 4A) and continued progressing both caudally and rostrally up to 33–49 weeks post-grafting, reaching strikingly long distances from the injection

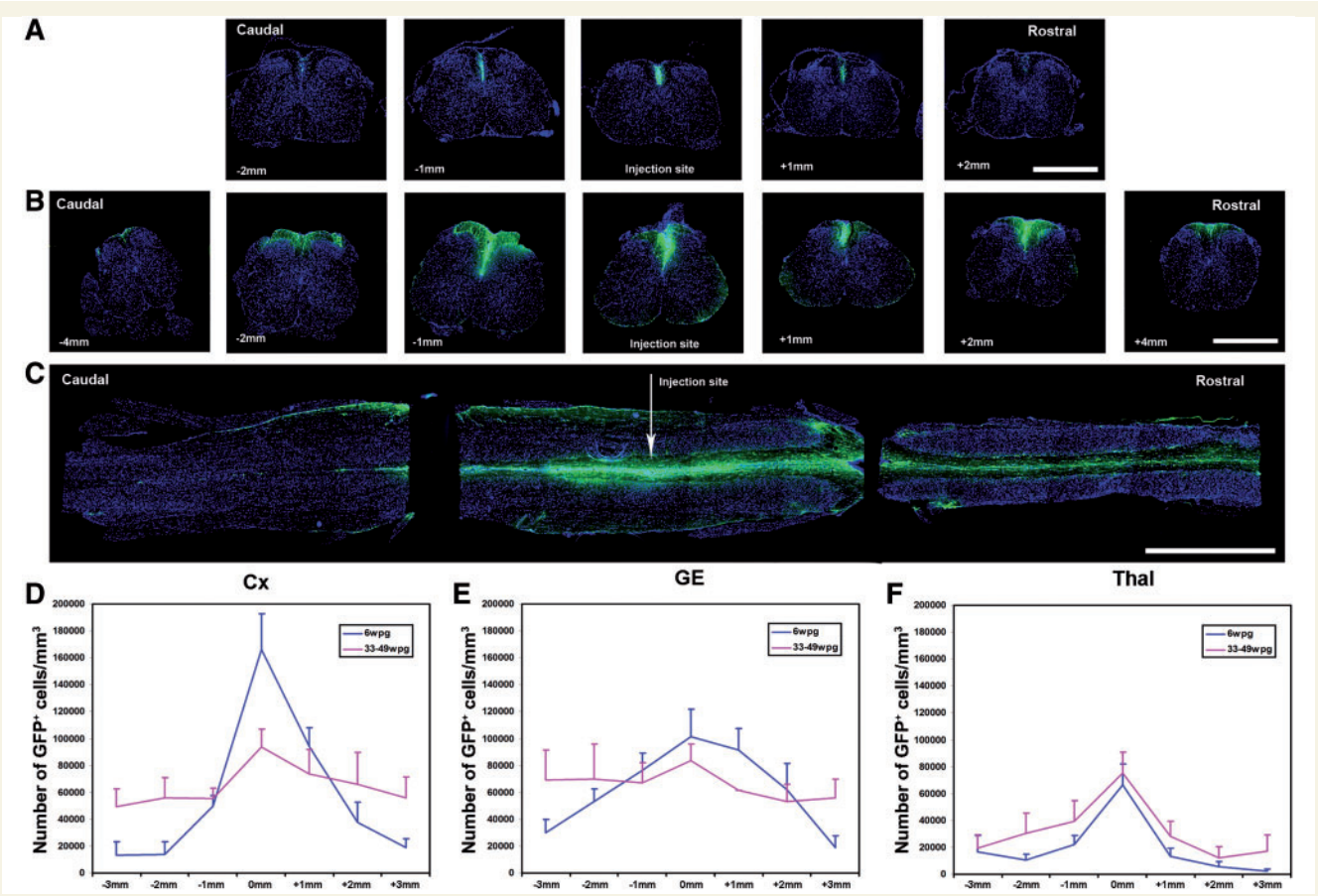

Figure 4 Grafted human foetal neural progenitor cells migrate caudally and rostrally from the injection site and progressively colonize the spinal cord white matter. (**A**) Coronal sections at different rostro-caudal levels of the nude mouse spinal cord at 6 weeks post-grafting. (**B**) Coronal sections at different rostro-caudal levels of the nude mouse spinal cord at 33–49 weeks post-grafting. (**C**) Transverse section of the nude mouse spinal cord at the level of the dorsal funiculus. Native GFP (green) allows detection of the grafted hNPCs. Hoechst dye (blue) was used to label cell nuclei. (**D–F**) Density of engrafted cells from cortex (**D**), ganglionic eminences (**E**) and thalamus (**F**) as a function of the distance from the injection site, illustrating human cell dispersal at both 6 weeks post-grafting (blue curves) and 33–49 weeks post-grafting (pink curves). Densities were expressed as the number of GFP^+ cells/mm^3 dorsal funiculus tissue. Cx = cortex; GE = ganglionic eminences; Thal = thalamus; wpg = weeks post-grafting. Scale bars: (**A–B**) 1 mm; (**C**) 2 mm.

site (26.0 ± 1.8, 25.3 ± 2.8 and 22.6 ± 0.5 mm between the most rostral and the most caudal GFP^+ cells in cortex, ganglionic eminences and thalamus groups, respectively) (Fig. 3A and B, Supplementary Fig. 5B and C). Moreover, at 6 weeks post-grafting, GFP^+ cells were located almost exclusively within the dorsal funiculus (Fig. 4A) whereas, at 33–49 weeks post-grafting, they had also migrated ventrally, preferentially reaching ventral white matter (Figs 3C–E and 4B) and occasionally grey matter (Figs 3D, E, 4B and C). Thus, a single injection point allowed considerable colonization of the spinal cord by the grafted hNPCs.

Most interestingly, although the total distance of migration was similar among the three groups, cell dispersal did not occur according to the same pattern in cortex, ganglionic eminences and thalamus. The evaluation of human cell density, expressed as a function of the distance from the injection site (Fig. 4D–F), revealed that, at 6 weeks post-grafting, human cells from ganglionic eminences dispersed more efficiently than cells from cortex and thalamus (blue curves in Fig. 4D–F). At 33–49 weeks post-grafting (pink curves in Fig. 4D–F), cells from cortex and ganglionic eminences (Fig. 4D and E) were no longer concentrated around the injection site and displayed equivalent distribution. In contrast, cells from thalamus (Fig. 4F) remained concentrated around the injection site and displayed poorer dispersal. In addition, at both 6 and 33–49 weeks post-grafting, cells from thalamus (Fig. 4F) displayed poorer survival than cells from cortex (Fig. 4D) and ganglionic eminences (Fig. 4E). Thus, it appears that, after long-term amplification *in vitro*, hNPCs from the three regions retained some properties related to their territorial origins that might have influenced their migration potential *in vivo*.

Human foetal neural progenitor cells give rise to differentiated oligodendrocytes after grafting into demyelinated spinal cord

We then evaluated the ability of hNPCs to differentiate into the three main neural lineages. Astroglial differentiation of hNPCs

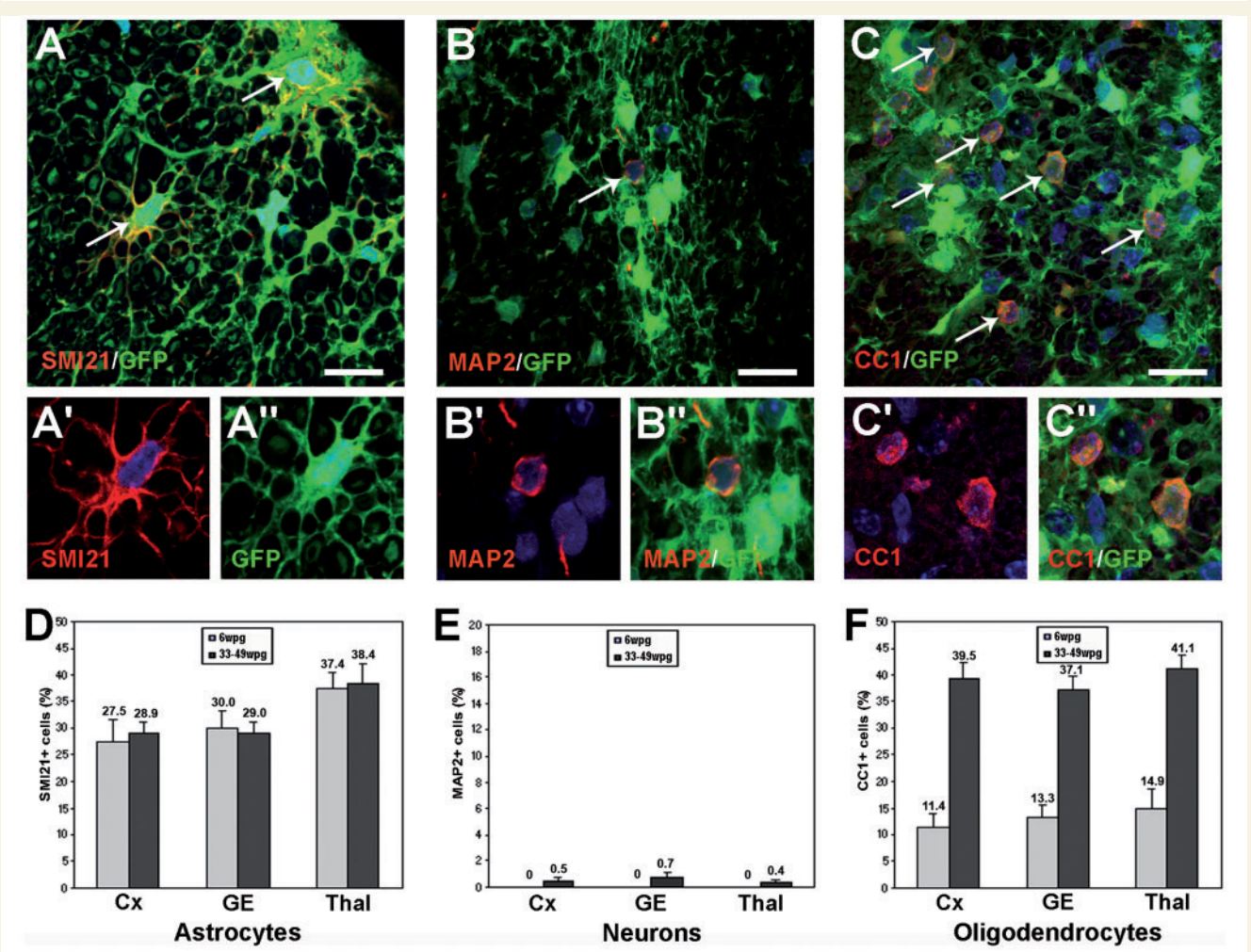

Figure 5 Human foetal neural progenitor cells display multipotency after transplantation into the demyelinated spinal cord of nude mice. (**A**) Anti-human GFAP(SMI21) immunostaining (red), showing hNPC-derived GFP$^+$ astrocytes (green, arrows). (**A′** and **A″**) Magnification of **A**. (**B**) Anti-MAP2 immunostaining (red), showing an hNPC-derived GFP$^+$ neuron (arrow). (**B′** and **B″**) Magnification of **B**. (**C**) Anti-APC(CC1) immunostaining (red), showing hNPC-derived GFP$^+$ oligodendrocytes (arrows). (**C′** and **C″**) Magnification of **C**. (**D–F**) Quantification of hNPC-derived GFAP(SMI21)$^+$ astrocytes (**D**), MAP2$^+$ neurons (**E**) and APC(CC1)$^+$ oligodendrocytes (**F**), expressed as the percentage of positive cells among GFP$^+$ cell population, at 6 weeks post-grafting (grey bars) and 33–49 weeks post-grafting (black bars). Cx = cortex; GE = ganglionic eminences; Thal = thalamus; wpg = weeks post-grafting. Scale bars: (**A–C**) 10 μm.

was revealed by the consistent expression of human-specific GFAP (SMI21) in every group (Fig. 5A and D) at both 6 weeks post-grafting (27.5 ± 4.1, 30.0 ± 3.3 and 37.4 ± 3.2% in cortex, ganglionic eminences and thalamus groups, respectively) and 33–49 weeks post-grafting (28.9 ± 2.2, 29.0 ± 2.2 and 38.4 ± 3.8% in cortex, ganglionic eminences and thalamus groups, respectively). Neuronal differentiation was assessed by anti-MAP2, anti-NeuN and anti-human Tau immunostaining. MAP2 was not detected at 6 weeks post-grafting (Fig. 5E), but was expressed by a few GFP$^+$ human cells at 33–49 weeks post-grafting (0.5 ± 0.2, 0.7 ± 0.4 and 0.4 ± 0.2% in cortex, ganglionic eminences and thalamus groups, respectively) (Fig. 5B and E), indicating that, after grafting into the demyelinated white matter, hNPCs differentiated into neurons to an extremely limited extent. This was further suggested by the absence of NeuN staining at both time points tested. Numerous Tau$^+$ cells were nevertheless observed at 6 and 33–49 weeks post-grafting (Fig. 6F). While Tau immunoreactivity may reveal the presence of either neuronal or oligodendroglial cells (LoPresti *et al.*, 1995; LoPresti, 2002), the absence of NeuN staining, the small number of MAP2$^+$/GFP$^+$ cells and the multipolar morphology of Tau$^+$ cells (Fig. 6F) suggested that the vast majority of the latter were in fact oligodendrocytes.

The ability of hNPCs to differentiate into mature oligodendrocytes *in vivo* was confirmed with other oligodendroglial markers. At 6 weeks post-grafting, APC(CC1) was expressed by 11.4 ± 2.4, 13.3 ± 2.3 and 14.9 ± 3.8% of GFP$^+$ cells in cortex, ganglionic eminences and thalamus groups, respectively, without any significant differences among the three groups (Fig. 5F). At 33–49 weeks post-grafting, the percentage of GFP$^+$ cells expressing APC(CC1) (Figs 5C and 6A) increased nearly 4-fold and reached 39.5 ± 2.9, 37.1 ± 2.5 and 41.1 ± 2.5% in cortex, ganglionic eminences and thalamus groups, respectively (Fig. 5F). Human NOGO-A (Fig. 6B), Olig2 (Fig. 6D) and Sox10 (Fig. 6E) were also

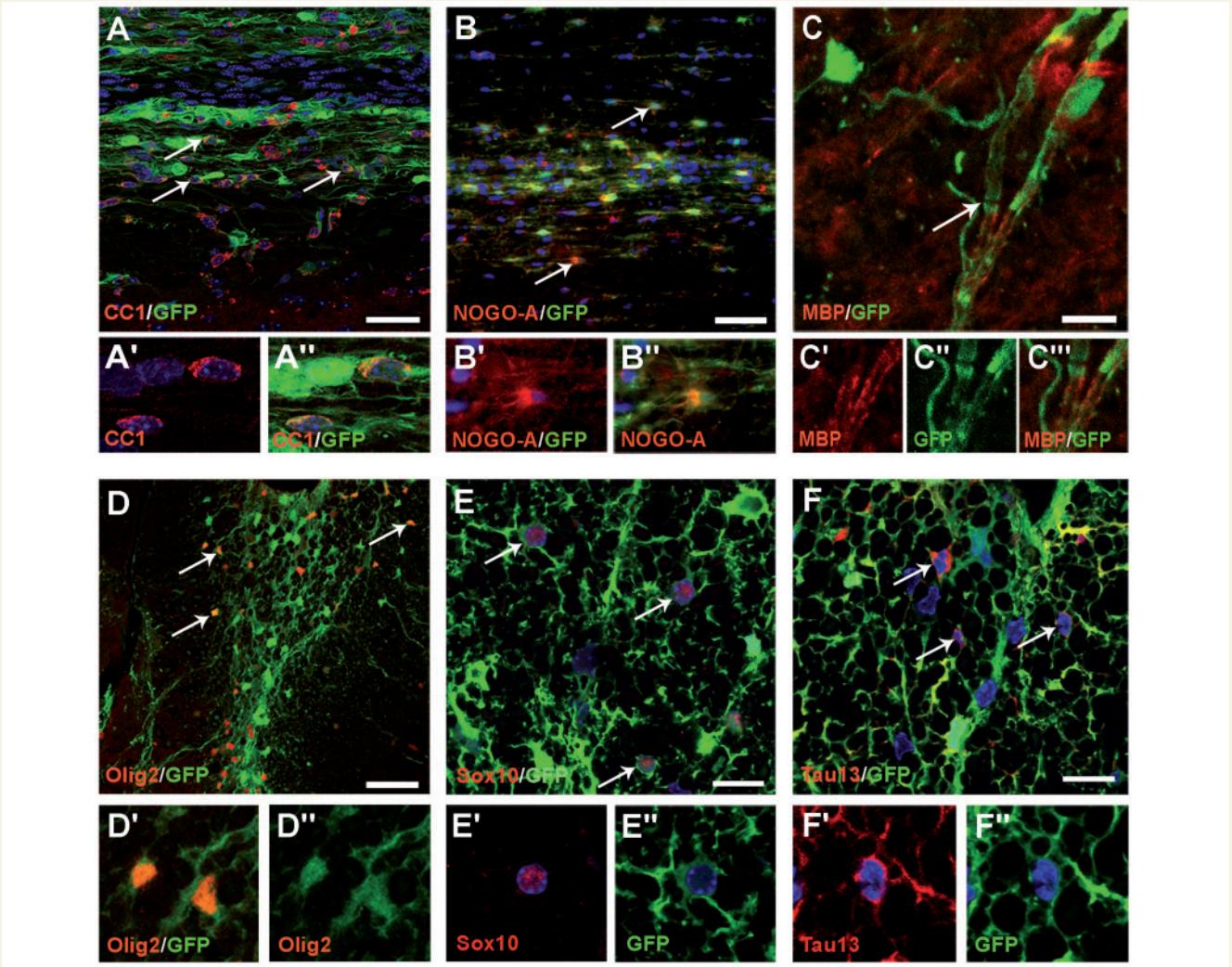

Figure 6 Human foetal neural progenitor cells from cortex, ganglionic eminences and thalamus give rise to mature oligodendrocytes after transplantation into the demyelinated spinal cord of nude mice. (**A–E**) Oligodendrocyte differentiation was confirmed by APC(CC1) (red, **A**), human NOGO-A (red, **B**), MBP (red, **C**) Olig2 (red, **D**) and Sox10 (red, **E**) labelling on sagittal (**A** and **B**) and coronal (**C–E**) sections. (**C**) Some GFP$^+$ cells extended long processes that wrapped around axons, co-expressed MBP and formed node of Ranvier-like structures (arrow). (**F**) Human Tau (Tau13) immunolabelling (red) on coronal sections, showing hNPC-derived GFP$^+$ cells (green) with oligodendroglial multipolar morphology (arrows). (**A′** and **A″**) Magnification of **A**; (**B′** and **B″**) magnification of **B**; (**C′–C″**) magnification of **C**; (**D′** and **D″**) magnification of **D**; (**E′** and **E″**) magnification of **E**; (**F′** and **F″**) magnification of **F**. Scale bars: (**A**) 50 μm; (**B**) 100 μm; (**C**) 10 μm; (**D**) 100 μm; (**E–F**) 10 μm.

expressed among the GFP$^+$ cell populations. Moreover, some multipolar GFP$^+$ cells extended long processes that enwrapped axons, expressed MBP and formed node of Ranvier-like structures (Fig. 6C), thereby strongly suggesting that at least some of the differentiated oligodendrocytes could form myelin.

Human neural progenitor cells from cortex, ganglionic eminences and thalamus form compact myelin in adult 'shiverer' mouse spinal cord

Cytoplasmic GFP is generally excluded from compact myelin, thus rendering remyelination by exogenous cells difficult to appreciate in wild-type animals. Human NPCs from cortex, ganglionic eminences and thalamus were therefore grafted into the focally demyelinated spinal cord of adult 'shiverer' mice that lack MBP expression and display uncompacted myelin at the ultrastructural level, thus allowing detection of donor-derived oligodendrocytes. Animals were sacrificed as late as possible given their lifespan (at 10.5 weeks post-grafting) and used for both immunohistochemical and ultrastructural analysis. Consistent expression of MBP (Fig. 7B–J) and human NOGO-A (Fig. 7F–H) confirmed the ability of hNPCs to give rise to myelinating oligodendrocytes. Interestingly, the MBP expression pattern indicated that, as in nude mice, human cells migrated over long distances (up to 8.5 mm) along the rostro-caudal axis (Fig. 7A and B) and were

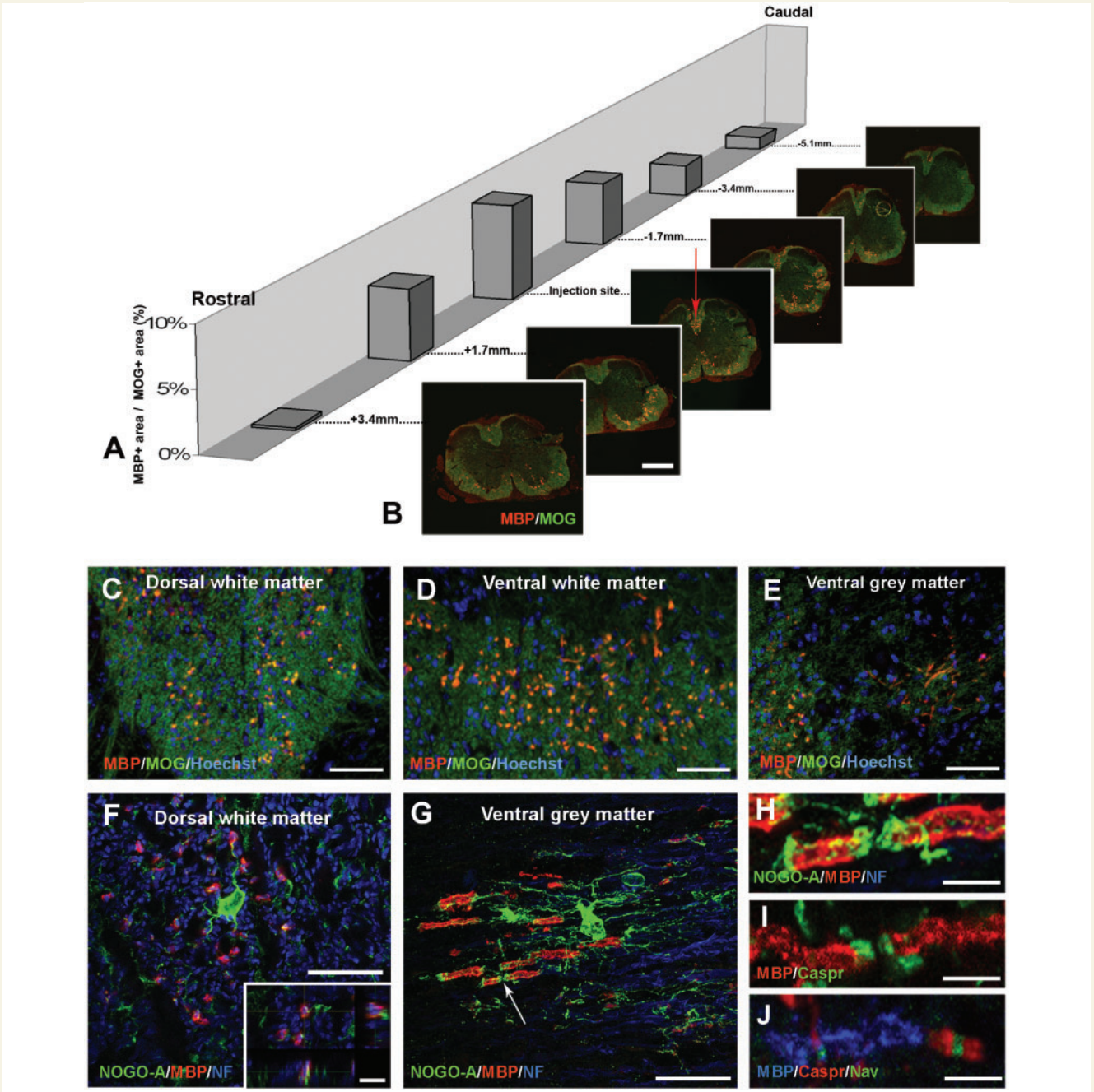

Figure 7 Human foetal neural progenitor cells give rise to myelinating oligodendrocytes after transplantation into the demyelinated spinal cord of 'shiverer' mice. (**A**) hNPC-derived myelination was quantified at different rosto-caudal levels of the 'shiverer' spinal cord and expressed as the percentage of MBP^+ area on MOG^+ white matter area. The largest extent of MBP^+ myelin was found at the level of the injection site (0 mm), reaching up to $8.11 \pm 0.71\%$ of the whole white matter. (**B–E**) Immunohistochemical labelling against MBP (red) and myelin oligodendrocyte glycoprotein (green), illustrating human-derived myelination of the 'shiverer' spinal cord at different rostro-caudal levels (**B**), as well as in dorsal funiculus (**C**), ventral white matter (**D**) and ventral grey matter (**E**). (**F–G**) Triple immunohistochemical labelling against MBP (red), human NOGO-A (green) and NF-200 (blue), showing multipolar hNPC-derived mature oligodendrocytes extending processes that enwrap and myelinate axons in dorsal white matter (**F**) and ventral grey matter (**G** and **H**). (**H**) magnification of **G** showing MBP^+ internodes and typical node of Ranvier structure. (**I**) Double immunohistochemical labelling against MBP (red) and Caspr (green) showing MBP^+ internodes and $Caspr^+$ paranodes. (**J**) Triple immunohistochemical staining against MBP (blue), Caspr (red) and pan-Na_v (green) showing that MBP^+ internodes participate in the clustering of Caspr and Na_v channels at the nodes of Ranvier, thereby suggesting that hNPC-derived myelin was functional. Scale bars: (**B**) 200 μm; (**C–E**) 50 μm; (**F**) 20 μm; (inset in **F**, **H–J**) 5 μm; (**G**) 10 μm.

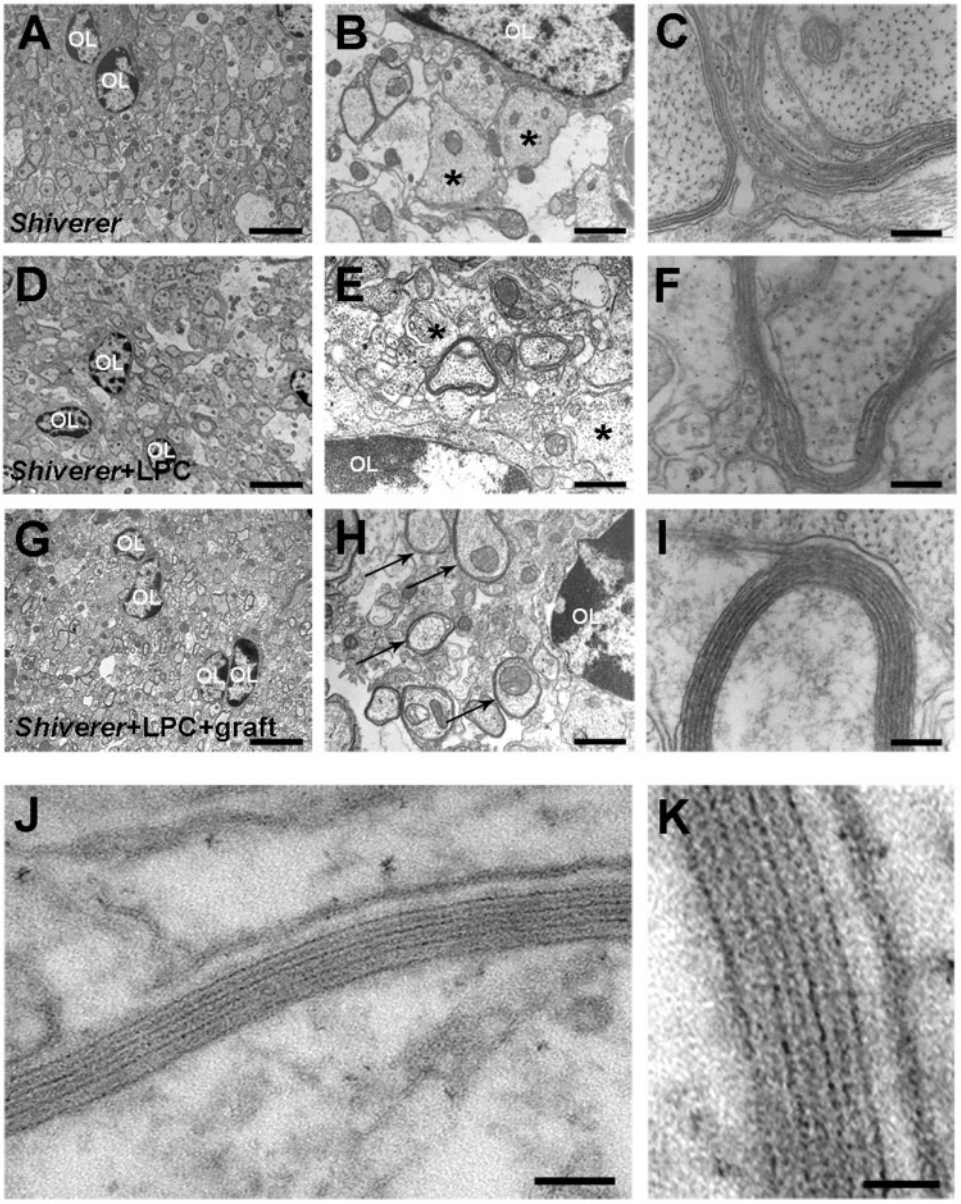

Figure 8 After hNPC transplantation into the demyelinated spinal cord of 'shiverer' mice, donor-derived oligodendrocytes display myelin compaction at the ultrastructural level. Ultrastructural analysis of myelin compaction in: (**A–C**) control 'shiverer' mice with neither lesion nor graft; (**D–F**) control 'shiverer' mice with lesion but no graft; and (**G–K**) 'shiverer' mice with lesion and hNPC graft. In controls (**A–F**), axons were either enwrapped with loose myelin (**C** and **F**) or non-myelinated (asterisks in **B** and **E**), and no compact myelin was observed. Regular myelin sheaths (**I**, arrows in **H**) and compact myelin (**J–K**) were observed only in grafted animals. OL = oligodendrocyte. Scale bars: (**A**, **D** and **G**) 5 μm; (**B**, **E** and **H**) 1 μm; (**C**, **F** and **I**) 250 nm; (**J**) 50 nm; (**K**) 20 nm.

not only present in the dorsal funiculus (Fig. 7B, C and F), but also in the ventral white matter (Fig. 7B and D) and less frequently in the grey matter (Fig. 7E and G). The extent of hNPC-derived myelination was assessed on coronal spinal cord sections by estimating the ratio of MBP^+ area on MOG^+ white matter area at different rostro-caudal levels (Fig. 7A). This measurement showed that up to $8.1 \pm 0.7\%$ of the white matter could be myelinated by human cells at the injection level. Confocal analysis showed that NOGO-A^+ cells extended multipolar processes that enwrapped NF^+ axons (Fig. 7F and G), formed MBP^+ internodes (Fig. 7G–J) and typical node of Ranvier-like structures (Fig. 7H). Most interestingly, the clustering of Caspr at the paranodes (Fig. 7I and J) and of Na_v channels at the nodes of Ranvier (Fig. 7J) further suggested the functionality of donor-derived myelin.

Animals were also used for ultrastructural analysis of myelin compaction. In control 'shiverer' mice that received neither lysolecithin injection nor graft (Fig. 8A–C), as well as in animals that received lysolecithin injection but no graft (Fig. 8D–F), the vast majority of axons were either non-myelinated (Fig. 8B and E) or enwrapped with loose myelin displaying large cytoplasmic

inclusions (Fig. 8C and F) and compact myelin sheaths were not observed. In animals that received both lysolecithin injection and hNPC graft (Fig. 8G–K), normal myelin sheaths with alternate major dense lines and intermediate lines (Fig. 8J–K) were observed, thus demonstrating unambiguously that hNPCs from foetal cortex, ganglionic eminences and thalamus differentiated into mature oligodendrocytes with the ability to form compact myelin around host axons.

Discussion

In the present study, we combined *in situ*, *in vitro* and *in vivo* studies to highlight the oligodendrogenic potential of different human foetal forebrain regions. We showed for the first time that the initial wave of oligodendrocyte progenitor cell emergence onsets as early as 7.5 weeks of gestation in the ventral telencephalon. Compartmentalization of the forebrain during that early window of development allowed consistent enrichment in putative oligodendrocyte progenitor cells *in vitro* after isolation of ganglionic eminences, as compared with cortex and thalamus. Finally, transplantation of hNPCs into two different models of focal gliotoxic demyelination demonstrated the great potential of cells isolated from these three regions to survive, migrate and successfully remyelinate the adult spinal cord.

Developmental biology has been widely used to understand normal and pathological oligodendrogenesis in the rodent CNS (Woodruff *et al*., 2001; Peru *et al*., 2006; Costa *et al*., 2009). Despite the scarcity of human embryonic and foetal tissue, ongoing efforts to understand human CNS development have allowed the establishment of many inter-species highly conserved mechanisms between human and rodent oligodendrogenesis (Hajihosseini *et al*., 1996; Grever *et al*., 1997; Back *et al*., 2001; Rakic and Zecevic, 2003; Chandran *et al*., 2004; Jakovcevski and Zecevic, 2005*a*, *b*). However, until now, the majority of data describing human oligodendrocyte development within the telencephalon were obtained from second trimester foetuses, at a time by which oligodendroglial cells had already spread within ventral and dorsal forebrain parenchyma (Rakic and Zecevic, 2003; Jakovcevski and Zecevic, 2005*a*, *b*). The paucity of earlier foetal tissue led to the erroneous idea that oligodendrocyte progenitor cell emergence might have larger sites of origin in human (the whole telencephalic ventricular zone) than in rodent forebrain (Jakovcevski and Zecevic, 2005*b*). Here, using earlier foetal brain tissue, we demonstrate for the first time that oligodendrocyte progenitor cell emergence onsets earlier than previously thought, after ~7.5 weeks of gestation. By that time, not only did the pattern of Olig2 expression closely resemble the one displayed by rodent CNS at embryonic Day 12.5 (Ligon *et al*., 2004; Rowitch, 2004; Richardson *et al*., 2006) but, in some cells emerging out of the ventricular zone, Olig2 expression was accompanied by Sox10 and platelet derived growth factor receptor α expression, indicating their belonging to the oligodendroglial lineage. As in rodents, oligodendrocyte progenitor cell emergence was restricted to medial ganglionic eminences and entopeduncular area, thus allowing the establishment of a close parallel between 7.5-week-old human foetuses and embryonic Day 12.5 rodent embryos in terms of oligodendrocyte lineage development. Consistent with our *in situ* study, immunocytochemical and reverse transcription-polymerase chain reaction analysis performed on forebrain dissociated cells indicated that Olig2 expression was prominent in ganglionic eminences. Moreover, the majority of $A2B5^+$ cells were identified as $MAP5^+$ neuroblasts in cortex and thalamus, whereas they mostly corresponded to early $MAP5^-$ glial progenitors in ganglionic eminences. This indicates that the isolation of a specific brain region allowed enrichment of a specific cell type and that such a CNS compartmentalization may be of potential benefit for oligodendroglial differentiation and myelin repair.

While necessary for the achievement of large-scale cultures, long-term *in vitro* amplification nevertheless induced major changes in the phenotypes of cells from the three regions. The most noticeable included: (i) an increase in Olig2 expression in cortex and thalamus groups, two dorsal regions where Olig2 was barely detectable *in vitro* at the time of explantation; (ii) a significant decrease in neuroblast proportions in the three groups; and (iii) a large increase in immature $Nestin^+/GFAP^-$ cell proportions. Moreover, consistent with previous studies (Roy *et al*., 1999; Zhang *et al*., 2000; Chandran *et al*., 2004), spontaneous generation of oligodendrocytes was not observed in any of the three groups. Most of these observations may be related to the effects of basic fibroblast growth factor, which has been widely used, alone or in combination with epidermal growth factor, for NPC amplification (Buc-Caron, 1995; Svendsen *et al*., 1998; Carpenter *et al*., 1999; Palmer *et al*., 2001; Buchet *et al*., 2002*b*). Indeed, it has been shown that basic fibroblast growth factor deregulates dorso-ventral patterning of embryonic rodent spinal cord progenitors (Gabay *et al*., 2003) in part by inducing Olig2 expression in dorsal progenitors. Moreover, basic fibroblast growth factor exposure induces Olig2 expression in human embryonic stem cell-derived NPCs (Hu *et al*., 2009) but prevents these cells from differentiating into motoneurons. Finally, basic fibroblast growth factor represses the transition between the $Olig2^+$ pre-oligodendrocyte progenitor cell stage towards the oligodendrocyte progenitor cell stage by disrupting Shh-dependent co-expression of Olig2 and Nkx2.2 (Hu *et al*., 2009), thereby explaining the scarcity of oligodendrocyte progenitor cells and mature oligodendrocytes in foetal hNPC cultures (Roy *et al*., 1999; Zhang *et al*., 2000; Chandran *et al*., 2004). Thus, neuroepithelial cell selection, attended by deregulation of Olig2 expression, inhibition of neuroblast commitment and inhibition of pre-oligodendrocyte progenitor cell to oligodendrocyte progenitor cell stage transition, might have induced enrichment in pre-oligodendrocyte progenitor cells in our cultures. This enrichment in immature $Olig2^+$ cells may be, at least in part, responsible for the fact that these cells generated large numbers of mature oligodendrocytes after grafting, irrespective of their territorial origins and despite their amplification *in vitro*.

Two demyelination paradigms were used to assess the remyelinating abilities of hNPCs from each region *in vivo*. After grafting into the demyelinated spinal cord of adult nude mice, hNPCs from cortex, ganglionic eminences and thalamus survived almost 1 year, by which time they had completely stopped proliferating. Most importantly, tumour formation was not observed at any time point after grafting. The limited lifespan of 'shiverer' mice did

not allow such a long-term analysis, but this second model was conclusively used to attest for newly formed myelin compaction. Remarkably, in both models, a single injection point was sufficient for extensive migration of the grafted hNPCs throughout the adult spinal cord white matter, and this migration occurred in both a rostro-caudal and dorso-ventral manner. Widespread migration with eventual chimerization of host rodent CNS was reported when foetal hNPCs/glial progenitors were grafted into the embryonic (Brustle *et al*., 1998) or newborn brain (Gumpel *et al*., 1987; Flax *et al*., 1998; Windrem *et al*., 2008), thereby allowing donor cells to benefit from guidance cues present in the developing CNS. Nonetheless, entire colonization of the host tissue required large entry routes, such as the ventricular system (Brustle *et al*., 1998; Flax *et al*., 1998), or multiple injection sites (Windrem *et al*., 2008), as well as large numbers of donor cells (Brustle *et al*., 1998; Windrem *et al*., 2008). On the contrary, when foetal hNPCs (Fricker *et al*., 1999) or adult human glial progenitor cells (Windrem *et al*., 2002) were focally injected into the adult parenchyma, they generally displayed more limited migration. Surprisingly, in our study, a single focal injection of a limited number of cells was sufficient to allow long-distance migration of the hNPCs, despite the less permissive adult environment. This striking ability of early foetal hNPCs to colonize the host adult CNS is probably related to both the immaturity of the donor cells and their intrinsic differentiation tempo. Previous studies have demonstrated that human foetal glial progenitors display a greater migratory potential and slower differentiation when isolated from late gestation foetal tissue than from the adult brain (Windrem *et al*., 2004). This study, therefore, suggested that the earlier the human glial progenitors were obtained, the greater their migratory potential was, even though they were isolated according to the same criteria and with the same technique. Here, hNPCs were isolated at a very early stage of development and amplified *in vitro*, a process that reinforced the immaturity of the donor cells. Moreover, the temporal increase in donor-derived APC(CC1)$^+$ mature oligodendrocytes and, to a lesser extent, of MAP2$^+$ neurons after grafting indicated that hNPC differentiation was a slow process. Consistent with this observation, *in vitro* studies showed that human embryonic stem cells display a much longer differentiation process than their rodent counterparts (Izrael *et al*., 2007; Hu *et al*., 2009). Thus, the great immaturity of the cells at the time of grafting, as well as their species-related slow differentiation, may account for their extensive migratory potential. In addition, this potential was not lowered by donor-derived astrocytes, which never appeared to form a glial scar. Our study, therefore, provides a paradigm by which the number of injection points can be limited and holds great promise for the treatment of CNS pathologies where donor cell migration is required.

The extensive migration of the hNPCs within the host parenchyma indicates that grafted cells did not specifically target the focally demyelinated area. Nevertheless, despite the absence of demyelinating cues outside the lesion, human cells actually produced myelin at long distances from their injection site, in both nude and 'shiverer' mice. In 'shiverer' mice, endogenous dysmyelination and altered oligodendrocyte–neuron interactions may account for the ability of the donor cells to replace endogenous oligodendrocytes. This has also been suggested by Windrem *et al*. (2008), who virtually induced 'humanization' of the 'shiverer' brain by transplanting second trimester foetal human glial progenitor cells in neonates. In their study, the authors discuss the possibility that human cells display a competitive strength over endogenous progenitors during post-natal development. Here, the fact that hNPCs were grafted into the adult spinal cord more likely implies replacement of the host deficient oligodendrocytes rather than competition with endogenous progenitors. It is possible that the grafted hNPCs took advantage of the increasing number of demyelinated axons in the ageing adult 'shiverer' CNS. Furthermore, we cannot rule out the possibility that hNPCs displayed an 'aggressive' behaviour towards host oligodendrocytes and then myelinated the axons they had themselves contributed to demyelinate. Either way, although post-natal 'shiverer' mice have been widely used as a paradigm to assess myelinating abilities of various cell types (Gumpel *et al*., 1987; Yandava *et al*., 1999; Nistor *et al*., 2005; Izrael *et al*., 2007; Windrem *et al*., 2008), very few studies documented these features in the adult 'shiverer' CNS, at a time by which the pathology has already settled (Cummings *et al*., 2005; Eftekharpour *et al*., 2007). Moreover, neither the extent of remyelination nor the migration achieved by the grafted cells were evaluated. Here, we show that NPCs of human origin are able to migrate extensively and produce myelin outside the temporal window of post-natal myelination, when developmental cues are no longer present, thereby offering the hope that genetic diseases with long-term molecular abnormalities, such as leucodystrophies, can be successfully reversed after the establishment of the pathology.

The situation in nude mice is more puzzling. Whether hNPCs myelinate unmyelinated axons of the spinal cord or replace formerly existing, healthy oligodendrocytes is unclear. It is now well-established that the adult parenchyma contains proliferating glial progenitors (Nishiyama *et al*., 2009) that participate in remyelination when demyelination occurs (Franklin and ffrench-Constant, 2008). Under normal conditions, the majority of these proliferating cells eventually die, while some (~5%) give rise to mature oligodendrocytes (Horner *et al*., 2000), thereby pleading in favour of a natural, albeit slow, turnover of myelinating oligodendrocytes in the adult CNS (Lasiene *et al*., 2009). In the present study, it is likely that hNPCs participated in this turnover in the mouse CNS. However, the existence of such a process remains a subject of debate, since myelinating oligodendrocyte replacement would imply a transitional 'nakedness' of axons.

Altogether, our data provide a link between developmental biology and experimental cell therapy, and reveal that early foetal hNPCs may offer new hope for the treatment of myelin affections. Although the functional equivalence of oligodendrocytes emerging from different CNS regions during development remains an open issue (Richardson *et al*., 2006), we show that hNPCs isolated from different forebrain areas can replace oligodendrocytes lost in demyelinating diseases with equal efficiency. Recently, oligodendrocyte progenitor cell derivation has been achieved from novel, virtually unlimited cell sources, such as human embryonic stem cells (Izrael *et al*., 2007; Hu *et al*., 2009) and induced pluripotent stem cells (Hu *et al*., 2010). However, as tissue-derived stem/progenitor cells, foetal hNPCs present the clear advantage over pluripotent cells to be 'neurally committed' and to lack

tumourigenicity after grafting. Hence, to date, foetal hNPCs still represent one of the safest means to achieve cell replacement in CNS diseases, and going thoroughly into the knowledge of their biological properties remains one of the key issues for efficient cell therapy of myelin affections. The present study provides a paradigm by which foetal hNPCs can be amplified *in vitro*, thereby giving rise to large-scale donor cells, before achieving extensive remyelination of the CNS without the need of oligodendrocyte progenitor cell selection or multiple injections. Therefore, our work sheds some new light on early oligodendrogenesis in the human forebrain and puts forward early foetal hNPCs as an efficient tool to carry out successful remyelination of the adult CNS.

Acknowledgements

We thank Dr Vanja Tepavcevic for her precious advice on animal surgery and electron microscopy; Dr Jacques Mallet for his generous gift of the CMV-GFP lentiviral vector; Dr Dominique Languy and Dr Aurélien Dauphin from the Pitié Salpêtrière Imaging Facility for their help in electron microscopy and confocal imaging; Christelle Enond and Elizabeth Huc for animal care.

Funding

Institut National de la Santé et de la Recherche Médicale (INSERM), Université Pierre et Marie Curie, European Leucodystrophy Association (ELA), National Multiple Sclerosis Society (NMSS, USA) and the European Programme (FP7-Health-F2-2010-241622); ELA; Association pour l'Education Thérapeutique et la Réadaptation des Enfants Infirmes Moteurs Cérébraux (APETREIMC); La Fondation Motrice and Institut pour la Recherche sur la Moelle épiniére et l'Encéphale (IRME) (fellowship to D.B.); INSERM (fellowship to C.G.); Contrat d'Interface Assistance Publique-Hôpitaux de Paris (AP-HP) (to A.B.-V.E. and B.N.O.).

Supplementary material

Supplementary material is available at *Brain* online.

References

Back SA, Luo NL, Borenstein NS, Levine JM, Volpe JJ, Kinney HC. Late oligodendrocyte progenitors coincide with the developmental window of vulnerability for human perinatal white matter injury. J Neurosci 2001; 21: 1302–12.

Brustle O, Choudhary K, Karram K, Huttner A, Murray K, Dubois-Dalcq M, et al. Chimeric brains generated by intraventricular transplantation of fetal human brain cells into embryonic rats. Nat Biotechnol 1998; 16: 1040–4.

Buc-Caron MH. Neuroepithelial progenitor cells explanted from human fetal brain proliferate and differentiate in vitro. Neurobiol Dis 1995; 2: 37–47.

Buchet D, Baron-Van Evercooren A. In search of human oligodendroglia for myelin repair. Neurosci Lett 2009; 456: 112–9.

Buchet D, Buc-Caron MH, Sabate O, Lachapelle F, Mallet J. Long-term fate of human telencephalic progenitor cells grafted into the adult mouse brain: effects of previous amplification in vitro. J Neurosci Res 2002a; 68: 276–83.

Buchet D, Serguera C, Zennou V, Charneau P, Mallet J. Long-term expression of beta-glucuronidase by genetically modified human neural progenitor cells grafted into the mouse central nervous system. Mol Cell Neurosci 2002b; 19: 389–401.

Carpenter MK, Cui X, Hu ZY, Jackson J, Sherman S, Seiger A, et al. In vitro expansion of a multipotent population of human neural progenitor cells. Exp Neurol 1999; 158: 265–78.

Chandran S, Caldwell M, Allen N. Introduction: stem cells and brain repair. Philos Trans R Soc Lond B Biol Sci 2008; 363: 5–7.

Chandran S, Compston A, Jauniaux E, Gilson J, Blakemore W, Svendsen C. Differential generation of oligodendrocytes from human and rodent embryonic spinal cord neural precursors. Glia 2004; 47: 314–24.

Costa MR, Bucholz O, Schroeder T, Gotz M. Late origin of glia-restricted progenitors in the developing mouse cerebral cortex. Cereb Cortex 2009; 19 (Suppl 1): i135–43.

Cummings BJ, Uchida N, Tamaki SJ, Salazar DL, Hooshmand M, Summers R, et al. Human neural stem cells differentiate and promote locomotor recovery in spinal cord-injured mice. Proc Natl Acad Sci USA 2005; 102: 14069–74.

Duncan ID. Replacing cells in multiple sclerosis. J Neurol Sci 2008; 265: 89–92.

Eftekharpour E, Karimi-Abdolrezaee S, Wang J, El Beheiry H, Morshead C, Fehlings MG. Myelination of congenitally dysmyelinated spinal cord axons by adult neural precursor cells results in formation of nodes of Ranvier and improved axonal conduction. J Neurosci 2007; 27: 3416–28.

Flax JD, Aurora S, Yang C, Simonin C, Wills AM, Billinghurst LL, et al. Engraftable human neural stem cells respond to developmental cues, replace neurons, and express foreign genes. Nat Biotechnol 1998; 16: 1033–9.

Franklin RJ, ffrench-Constant C. Remyelination in the CNS: from biology to therapy. Nat Rev Neurosci 2008; 9: 839–55.

Fricker RA, Carpenter MK, Winkler C, Greco C, Gates MA, Bjorklund A. Site-specific migration and neuronal differentiation of human neural progenitor cells after transplantation in the adult rat brain. J Neurosci 1999; 19: 5990–6005.

Gabay L, Lowell S, Rubin LL, Anderson DJ. Deregulation of dorsoventral patterning by FGF confers trilineage differentiation capacity on CNS stem cells in vitro. Neuron 2003; 40: 485–99.

Goldman SA, Schanz S, Windrem MS. Stem cell-based strategies for treating pediatric disorders of myelin. Hum Mol Genet 2008; 17: R76–83.

Grever WE, Weidenheim KM, Tricoche M, Rashbaum WK, Lyman WD. Oligodendrocyte gene expression in the human fetal spinal cord during the second trimester of gestation. J Neurosci Res 1997; 47: 332–40.

Gumpel M, Lachapelle F, Gansmuller A, Baulac M, Baron van Evercooren A, Baumann N. Transplantation of human embryonic oligodendrocytes into shiverer brain. Ann N Y Acad Sci 1987; 495: 71–85.

Hajihosseini M, Tham TN, Dubois-Dalcq M. Origin of oligodendrocytes within the human spinal cord. J Neurosci 1996; 16: 7981–94.

Horner PJ, Power AE, Kempermann G, Kuhn HG, Palmer TD, Winkler J, et al. Proliferation and differentiation of progenitor cells throughout the intact adult rat spinal cord. J Neurosci 2000; 20: 2218–28.

Hu BY, Du ZW, Zhang SC. Differentiation of human oligodendrocytes from pluripotent stem cells. Nat Protoc 2009; 4: 1614–22.

Hu BY, Weick JP, Yu J, Ma LX, Zhang XQ, Thomson JA, et al. Neural differentiation of human induced pluripotent stem cells follows developmental principles but with variable potency. Proc Natl Acad Sci USA 2010; 107: 4335–40.

Izrael M, Zhang P, Kaufman R, Shinder V, Ella R, Amit M, et al. Human oligodendrocytes derived from embryonic stem cells: Effect of noggin

on phenotypic differentiation in vitro and on myelination in vivo. Mol Cell Neurosci 2007; 34: 310–23.

Jakovcevski I, Filipovic R, Mo Z, Rakic S, Zecevic N. Oligodendrocyte development and the onset of myelination in the human fetal brain. Front Neuroanat 2009; 3: 5.

Jakovcevski I, Zecevic N. Olig transcription factors are expressed in oligodendrocyte and neuronal cells in human fetal CNS. J Neurosci 2005a; 25: 10064–73.

Jakovcevski I, Zecevic N. Sequence of oligodendrocyte development in the human fetal telencephalon. Glia 2005b; 49: 480–91.

Kessaris N, Fogarty M, Iannarelli P, Grist M, Wegner M, Richardson WD. Competing waves of oligodendrocytes in the forebrain and postnatal elimination of an embryonic lineage. Nat Neurosci 2006; 9: 173–9.

Lasiene J, Matsui A, Sawa Y, Wong F, Horner PJ. Age-related myelin dynamics revealed by increased oligodendrogenesis and short internodes. Aging Cell 2009; 8: 201–13.

Ligon KL, Alberta JA, Kho AT, Weiss J, Kwaan MR, Nutt CL, et al. The oligodendroglial lineage marker OLIG2 is universally expressed in diffuse gliomas. J Neuropathol Exp Neurol 2004; 63: 499–509.

LoPresti P. Regulation and differential expression of tau mRNA isoforms as oligodendrocytes mature in vivo: implications for myelination. Glia 2002; 37: 250–7.

LoPresti P, Szuchet S, Papasozomenos SC, Zinkowski RP, Binder LI. Functional implications for the microtubule-associated protein tau: localization in oligodendrocytes. Proc Natl Acad Sci USA 1995; 92: 10369–73.

Maire CL, Buchet D, Kerninon C, Deboux C, Baron-Van Evercooren A, Nait-Oumesmar B. Directing human neural stem/precursor cells into oligodendrocytes by overexpression of Olig2 transcription factor. J Neurosci Res 2009; 87: 3438–46.

Martino G, Franklin RJ, Van Evercooren AB, Kerr DA. Stem cell transplantation in multiple sclerosis: current status and future prospects. Nat Rev Neurol 2010; 6: 247–55.

Murray K, Dubois-Dalcq M. Emergence of oligodendrocytes from human neural spheres. J Neurosci Res 1997; 50: 146–56.

Nishiyama A, Komitova M, Suzuki R, Zhu X. Polydendrocytes (NG2 cells): multifunctional cells with lineage plasticity. Nat Rev Neurosci 2009; 10: 9–22.

Nistor GI, Totoiu MO, Haque N, Carpenter MK, Keirstead HS. Human embryonic stem cells differentiate into oligodendrocytes in high purity and myelinate after spinal cord transplantation. Glia 2005; 49: 385–96.

Palmer TD, Schwartz PH, Taupin P, Kaspar B, Stein SA, Gage FH. Cell culture. Progenitor cells from human brain after death. Nature 2001; 411: 42–3.

Peru RL, Mandrycky N, Nait-Oumesmar B, Lu QR. Paving the axonal highway: from stem cells to myelin repair. Stem Cell Rev 2008; 4: 304–18.

Quinn SM, Walters WM, Vescovi AL, Whittemore SR. Lineage restriction of neuroepithelial precursor cells from fetal human spinal cord. J Neurosci Res 1999; 57: 590–602.

Rakic S, Zecevic N. Early oligodendrocyte progenitor cells in the human fetal telencephalon. Glia 2003; 41: 117–27.

Richardson WD, Kessaris N, Pringle N. Oligodendrocyte wars. Nat Rev Neurosci 2006; 7: 11–8.

Rowitch DH. Glial specification in the vertebrate neural tube. Nat Rev Neurosci 2004; 5: 409–19.

Roy NS, Wang S, Harrison-Restelli C, Benraiss A, Fraser RA, Gravel M, et al. Identification, isolation, and promoter-defined separation of mitotic oligodendrocyte progenitor cells from the adult human subcortical white matter. J Neurosci 1999; 19: 9986–95.

Spassky N, Goujet-Zalc C, Parmantier E, Olivier C, Martinez S, Ivanova A, et al. Multiple restricted origin of oligodendrocytes. J Neurosci 1998; 18: 8331–43.

Svendsen CN, ter Borg MG, Armstrong RJ, Rosser AE, Chandran S, Ostenfeld T, et al. A new method for the rapid and long term growth of human neural precursor cells. J Neurosci Methods 1998; 85: 141–52.

Tepavcevic V, Baron-Van Evercooren A. Transplantation of myelin-forming cells. In: Squire LR, editor. Encyclopedia of neuroscience. Oxford: Academic Press; 2008.

Windrem MS, Nunes MC, Rashbaum WK, Schwartz TH, Goodman RA, McKhann G 2nd. Fetal and adult human oligodendrocyte progenitor cell isolates myelinate the congenitally dysmyelinated brain. Nat Med 2004; 10: 93–7.

Windrem MS, Roy NS, Wang J, Nunes M, Benraiss A, Goodman R, et al. Progenitor cells derived from the adult human subcortical white matterdisperse and differentiate as oligodendrocytes within demyelinated lesions of the rat brain. J Neurosci Res 2002; 69: 966–75.

Windrem MS, Schanz SJ, Guo M, Tian GF, Washco V, Stanwood N, et al. Neonatal chimerization with human glial progenitor cells can both remyelinate and rescue the otherwise lethally hypomyelinated shiverer mouse. Cell Stem Cell 2008; 2: 553–65.

Woodruff RH, Tekki-Kessaris N, Stiles CD, Rowitch DH, Richardson WD. Oligodendrocyte development in the spinal cord and telencephalon: common themes and new perspectives. Int J Dev Neurosci 2001; 19: 379–85.

Yandava BD, Billinghurst LL, Snyder EY. "Global" cell replacement is feasible via neural stem cell transplantation: evidence from the dysmyelinated shiverer mouse brain. Proc Natl Acad Sci USA 1999; 96: 7029–34.

Zhang SC, Ge B, Duncan ID. Tracing human oligodendroglial development in vitro. J Neurosci Res 2000; 59: 421–9.